Inorg. Chem. **2007**, *46*, 11431–11436

Syntheses and Structural Characterization of a Series of One-Dimensional Fluorotitanophosphates $(NH_4)_xK_{4-x}[Ti_2PO_4F_9]$ ($x = 0$, 0.70, 1.00, 1.25)

Sihai Yang,[†] Guobao Li,*[,†] Lei Li,[†] Shujian Tian,[†] Fuhui Liao,[†] Ming Xiong,[‡] and Jianhua Lin*[,†]

Beijing National Laboratory for Molecular Sciences, State Key Laboratory of Rare Earth Materials Chemistry and Applications, College of Chemistry and Molecular Engineering, Peking University, Beijing 100871, P. R. of China, China University of Geoscience, X-ray Laboratory, Beijing 100083, P. R. China

Received July 9, 2007

A series of novel fluorotitanophosphates with a general formula $(NH_4)_xK_{4-x}[Ti_2PO_4F_9]$ ($x = 0$, 0.70, 1.00, 1.25, named as **1**, **2**, **3**, and **4** respectively) have been synthesized under hydrothermal conditions. Their structures were determined by X-ray single-crystal diffraction technique, which show that all of the phases in this series contain an idental anionic fluorotitanophosphate chain, consisting of alternating linkage of PO_4 tetrahedra and TiO_2F_4 octahedra. The fluorotitanophosphate chain is unique, which is different from the first titanophosphate chain found in $[Ti_3P_6O_{27}]\cdot 5[NH_3CH_2{-}CH_2NH_3]\cdot 2H_3O$. Another interesting observation of this series is that, by partial substitution of potassium by ammonium, the structure converts to a more-symmetric version, while maintaining all of the topological feature.

Introduction

Recently, considerable attentions are focused on titanium phosphates (TiPOx) because they are an important class of materials showing various tuneable physical properties and industrial applications, such as nonlinear optics,[1,2] ion exchange,[3] ion conductivity,[4] and redox catalysis.[5,6] A large number of new TiPOx with diverse structures have been reported. Most of them adopt 2D layers[7−17] and even 3D frameworks.[18−23] TiPOx with a 1D chain structure are rare, and only few examples, such as $[Ti_3P_6O_{27}]\cdot 5[NH_3CH_2CH_2NH_3]\cdot 2H_3O$[24] and $(NH_4)_2TiO[O_3P{-}(CH_2){-}PO_3]$,[25] were reported. However, as it is known, the structure of 1D TiPOx

* To whom correspondence should be addressed. Fax: 86-10-62753541. Tel: 86-10-62750342. E-mail: liguobao@pku.edu.cn (G.L), jhlin@pku.edu.cn (J.L.).

† Peking University.

‡ China University of Geoscience.

(1) Masse, R.; Grenier, J. C. *Bull. Soc. Fr. Mineral. Cristallogr.* **1971**, *94*, 437−439.
(2) Satyanarayan, M. N.; Deepthy, A.; Bhat, H. L. *Crit. Rev. Solid State Mater. Sci.* **1999**, *24*, 103−191.
(3) Allulli, S.; Ferragina, C.; La Ginestra, A.; Massucci, M. A.; Tomassini, N. *J. Inorg. Nucl. Chem.* **1977**, *39*, 1043−1048.
(4) Delmas, C.; Nadiri, A.; Soubeyroux, J. L. *Solid State Ionics* **1988**, *28*−*30*, 419−423.
(5) Serre, C.; Férey, G. *C. R. Acad. Sci., Ser. IIc* **1999**, *2*, 85−91.
(6) Ekambaram, S.; Serre, C.; Férey, G.; Sevov, S. C. *Chem. Mater.* **2000**, *12*, 444−449.
(7) Zhao, Y. N.; Zhu, G. S.; Jiao, X. L.; Liu, W.; Pang, W. Q. *J. Mater. Chem.* **2000**, *10*, 463−467.
(8) *Inorganic Ion Exchange Materials*; Clearfield, A., Ed.; CRC Press: Boca Raton, FL, 1982.
(9) Christensen, A. N.; Andersen, A. G. K.; Andersen, I. G. K.; Alberti, G.; Nielsen, M.; Lehmann, S. M. *Acta Chem. Scand.* **1990**, *44*, 865−872.
(10) Bruque, S.; Aranda, M. A. G.; Losilla, E. R.; Olivera-Pastor, P.; Maireles-Torres, P. *Inorg. Chem.* **1995**, *34*, 893−899.
(11) Salvado, M. A.; Garcia-Granda, S.; Rodriguez, J. *Mater. Sci. Forum* **1994**, *166*−*169*, 619−624.
(12) Serre, C.; Taulelle, F.; Férey, G. *Solid State Sci.* **2001**, *3*, 623−632.
(13) Mafra, L.; Paz, F. A. A.; Rocha, J.; Espina, A.; Khainakov, S. A.; García, J. R.; Fernandez, C. *Chem. Mater.* **2005**, *17*, 6287−6294.
(14) Liu, Y. L.; Shi, Z.; Fu, Y. L.; Chen, W.; Li, B. Z.; Hua, J.; Liu, W. Y.; Deng, F.; Pang, W. Q. *Chem. Mater.* **2002**, *1*, 1555−1563.
(15) Li, Y. J.; Whittingham, M. S. *Solid State Ionics* **1993**, *63*−*65*, 391−395.
(16) Bortun, A. I.; Bortun, L. N.; Clearfield, A.; Villa-Garcia, M. A.; Garcia, J. R.; Rodriguez, J. *J. Mater. Res.* **1996**, *11*, 2490−2498.
(17) Serre, C.; Férey, G. *J. Mater. Chem.* **1999**, *9*, 579−584.
(18) Poojary, D. M.; Bortun, A. I.; Bortun, L. N.; Clearfield, A. *J. Solid State Chem.* **1997**, *132*, 213−223.
(19) Ekambaram, S.; Sevov, S. C. *Angew. Chem., Int. Ed.* **1999**, *38*, 372−375.
(20) Fu, Y. L.; Liu, Y. L.; Shi, Z.; Zou, Y. C.; Pang, W. Q. *J. Solid State Chem.* **2001**, *162*, 96−102.
(21) Ekambaram, S.; Serre, C.; Férey, G.; Sevov, S. C. *Chem. Mater.* **2000**, *12*, 444−449.
(22) Liu, Y. L.; Shi, Z.; Zhang, L. R.; Fu, Y. L.; Chen, J. S.; Li, B. Z.; Hua, J.; Pang, W. Q. *Chem. Mater.* **2001**, *13*, 2017−2022.
(23) Yang, S. H.; Li, G. B.; You, L. P.; Tao, J. L.; Loong, C. K.; Tian, S. J.; Liao, F. H.; Lin, J. H. *Chem. Mater.* **2007**, *19*, 942−947.
(24) Guo, Y. H.; Shi, Z.; Yu, J. H.; Wang, J. D.; Liu, Y. L.; Bai, N.; Pang, W. Q. *Chem. Mater.* **2001**, *13*, 203−207.

10.1021/ic701715k CCC: $37.00
Published on Web 11/30/2007

can be considered as a kind of fundamental building unit for all TiPOx, because the 3D structures are composed of certain 2D layers, which could be further related to 1D chains. Therefore, TiPOx with new chain structures are very interesting not only for searching new materials but also for understanding the structural principle of these compounds. In this article, we report the syntheses and characterizations of a series of new 1D fluorotitanophosphates, $K_4[Ti_2PO_4F_9]$ (**1**), $(NH_4)_{0.7}K_{3.3}[Ti_2PO_4F_9]$ (**2**), $NH_4K_3[Ti_2PO_4F_9]$ (**3**), and $(NH_4)_{1.25}K_{2.75}[Ti_2PO_4F_9]$ (**4**).

Experimental Section

Synthesis. Single crystals of **1**, **2**, **3**, and **4** were obtained under hydrothermal conditions in Teflon-lined stainless-steel autoclaves, starting from acidic suspensions of K_2TiF_6 and phosphoric acid in a molar ratio of 2.0:1.0:7.0 (K/Ti/P). As a typical example, a mixture of 3.00 g (12.5 mmol) of K_2TiF_6 (C.R.) and 6.0 mL (87.6mmol) of H_3PO_4 (85%, A.R.), together with 6.0 mL (90.0mmol) of ethylenediamine ($H_2N(CH_2)_2NH_2$, A.R.) for **1**, or with 3.0 mL (52.5mmol) $N_2H_4{\cdot}H_2O$ (85%, A.R.) and 2.0 mL (30.0mmol) of $H_2N(CH_2)_2NH_2$ for **2**, or with 8.0 mL(52.0mmol) ammonia $NH_3{\cdot}H_2O$ (25%, A.R.) for **3**, or with 5.0 mL(87.5mmol) $N_2H_4{\cdot}H_2O$ for **4**, were charged into a 50 mL Teflon-lined stainless-steel autoclave. Ethylenediamine used in the synthesis of **1** could not be changed to $N_2H_4{\cdot}H_2O$ or $NH_3{\cdot}H_2O$. However, in the syntheses of **2**, **3**, and **4**, the use of $N_2H_4{\cdot}H_2O$ can be changed to $NH_3{\cdot}H_2O$ with a change of the amount, or vice versa. The autoclave was sealed, heated to 175 °C under autogenous pressure for 8 days, and then cooled to room temperature at a rate of 3 °C/h. About 2.00 g of product (yield 60% based on K_2TiF_6), appearing as needlelike single crystals, were isolated by washing the product with hot distilled water and dried at ambient temperature. **1**, **2**, **3**, and **4** are stable and insoluble in water and most organic solvents.

Characterization. The products were examined by X-ray diffraction on a Rigaku D/Max-2000 diffractometer with graphite monochromatized Cu Kα radiation at 40 kV and 100 mA or a Bruker D8 Advance diffractometer with Cu Kα1 ($\lambda = 1.54056$ Å) radiation at 50 kV and 40 mA. XRD powder patterns refined from single-crystal data using *GSAS*[26] software closely matched those obtained from bulk sample, indicating that a large amount of pure compounds can be obtained instead of only a few single crystals mixed in other phases (Supporting Information for typical data). The elemental ratio (K/Ti/P) was measured by inductively coupled plasma optical emission spectroscopy (ICP-OES) on a Varian Vista RL spectrometer with radial plasma observation. As a typical analytic process, **1**, **2**, **3**, or **4** was dissolved in acid (HCl) to appropriate concentration and then measured by ICP-OES for three parallel samples to calculate an average value. Elemental analyses of nitrogen and hydrogen were carried out on a Elementar Vario EL III microanalyzer. The ratio of F/O was measured by energy dispersive X-ray spectroscopy on an H-9000 transmission electron microscope with a value of about 1.7:1.0 (the calculated value is about 2.3:1.0, the more reliable studies on the amount of fluorine and oxygen in the compound are presented in the Supporting Information). The chemical elemental analysis results are listed in Table 1. IR spectra were recorded in the 400−4000 cm^{-1} range using a Magna-IR 750 FTIR spectrometer. Thermogravimetric−differential scanning calorimetry−mass spectrometric coupled analysis (TG−DSC−MS) was performed in a Netzsch STA 449C simultaneous analyzer utilizing Al_2O_3 crucibles and type-S thermocouples. The thermal stability was investigated up to 1073 K with TG−MS in a heating/cooling rate of 10 K/min in a dynamic argon atmosphere (gas flow 0.03 L/min).

Table 1. Chemical Elemental Analyses of **1**, **2**, **3**, and **4**

	K:Ti:P		N %		H %	
	calcd	found	calcd	found	calcd	found
1	4:2:1	3.9:2.1:1.0	0	0.3	0	0.4
2	3.3:2:1	3.4:2.1:1.0	1.95	1.97	0.60	1.02
3	3:2:1	3.0:2.2:1.0	2.82	2.84	0.81	1.04
4	2.75:2:1	2.6:2.2:1.0	3.56	3.34	1.02	1.16

Crystallographic Studies. Single crystals of **1**, **2**, **3**, and **4** (colorless, dimensions about $0.4 \times 0.2 \times 0.2$ mm^3) were carefully selected under an optical microscope and glued to thin glass fibers with epoxy resin. Intensity data of **1** and **2** were collected on a Rigaku AFC6S diffractometer with graphite monochromatic Mo Kα ($\lambda = 0.71073$ Å) radiation by using the ω-2θ scan method at room temperature. A PSI absorption correction was applied using the *teXsan* program.[27] Intensity data of **3** and **4** were collected on a Bruker *SMART* X-ray diffractometer, equipped with an APEX-CCD area detector and using graphite monochromatic Mo Kα ($\lambda = 0.71073$ Å) radiation at room temperature. The data absorption correction was applied based on symmetry-equivalent reflections using the *ABSOR* program.[28] The structures were solved with direct methods and refined on F^2 with full-matrix least-squares methods using *SHELXS-97*[29] and *SHELXL-97*[30] programs, respectively. All of the nonhydrogen atoms were refined anisotropically. The hydrogen atoms were added in the riding model and refined isotropically with N−H = 0.86 Å. The total occupancies of nitrogen in **2**−**4** phases were fixed at analytical values of the nitrogen element, as shown in Table 1. To find the suitable sites for the ammonium nitrogen atom, the occupancies of all three potassium atom sites in **2**−**4** were refined. In **2** and **3**, only the occupancy of K1 reduced observably after the refinement, so the ammonium nitrogen atom was set to the K1 site with proper ratio obtained from elemental analytical values. For **4**, the occupancies of both K1 and K3 sites reduced during the refinement, and then the ammonium nitrogen atom was fixed to the K1 and K3 sites with the proper ratio, the final relative ratio of the nitrogen atoms at the two sites were obtained by refinement. The crystallographic data and the structural refinement parameters for **1**, **2**, **3**, and **4** are summarized in Table 2. The corresponding bond lengths are listed in Table 3 (the atomic positions were listed in the Supporting Information). Further details of the crystal structures reported in this article can be obtained from the Fachinformationszentrum Karlsruhe, 76344 Eggenstein-Leopoldshafen, Germany, (fax: (49) 7247 808 666; e-mail: crysdata@fiz-karlsruhe.de) on quoting the depository numbers CSD-417917, 417987, 417918, and 417916.

Results

Infrared (IR) Spectra. The Fourier transform infrared (FTIR) micro-spectroscopy of **1**, **2**, **3**, and **4** is shown in

(25) Ninclaus, C.; Serre, C.; Riou, D.; Férey, G. *C. R. Acad. Sci., Ser. IIc* **1998**, *1*, 551.
(26) (a) Larson, A. C.; von Dreele, R. B. *Report LAUR 86−748*; Los Alamos National Laboratory, 1985. (b) Rietveld, H. M. *J. Appl. Crystallogr.* **1969**, *2*, 65.
(27) Molecular Structure Corporation, *TEXSAN, Single Crystal Structure Analysis Software*; MSC: The Woodlands, TX, U.S.A., 1995.
(28) Higashi, T. *ABSCOR, Empirical Absorption based on Fourier Series Approximation*; Rigaku Corporation, Tokyo, 1995.
(29) Sheldrick, G. M. *SHELXS97, Program for Solution o f Crystal Structures*; University of Göttingen: Göttingen, Germany, 1997.
(30) Sheldrick, G. M. *SHELXL97, Program for Solution o f Crystal Structures*; University of Göttingen: Göttingen, Germany, 1997.

Table 2. Crystallographic and Structural Refinement Parameters for **1**, **2**, **3**, and **4**

formula	$K_4[Ti_2PO_4F_9]$	$(NH_4)_{0.7}K_{3.3}[Ti_2PO_4F_9]$	$NH_4K_3[Ti_2PO_4F_9]$	$(NH_4)_{1.25}K_{2.75}[Ti_2PO_4F_9]$
fw	518.17	503.42	497.12	491.84
space group	$P2_1/n$	$P2_1/m$	$P2_1/m$	$P2_1/m$
a (Å)	5.8402(12)	5.8854(12)	5.8777(12)	5.8962(12)
b (Å)	11.000(2)	11.014(2)	10.991(2)	11.011(2)
c (Å)	19.436(4)	10.227(2)	10.219(2)	10.252(2)
β (deg)	90.87(3)	105.99(3)	106.04(3)	106.10(3)
V (Å^3)	1248.4(4)	637.3(2)	634.5(2)	639.5(2)
Z	4	2	2	2
d_{calcd} (g·cm^{-3})	2.757	2.623	2.602	2.554
T (K)	298	298	298	298
λ(Mo Kα) (Å)	0.71073	0.71073	0.71073	0.71073
GOF on F^2	1.000	1.000	1.000	1.000
μ (mm^{-1})	2.859	2.575	2.489	2.389
R_{int}	0.043	0.017	0.019	0.022
R1, wR2 (I > 2δ(I))	0.031, 0.075	0.047, 0.124	0.036, 0.088	0.031, 0.080
R1, wR2 (all data)	0.046, 0.086	0.050, 0.126	0.040, 0.090	0.034, 0.082

Table 3. Selected Bond Distances (Angstroms) for **1**, **2**, **3**, and **4**

bond	**1**	bond	**2**	**3**	**4**
Ti1−F1×2	1.863(2)	Ti1−F1×2	1.858(4)	1.855(2)	1.859(1)
Ti1−F2×2	1.863(2)	Ti1−F2×2	1.864(4)	1.855(2)	1.856(1)
Ti1−O2×2	1.929(2)	Ti1−O2×2	1.914(4)	1.918(2)	1.924(2)
Ti2−F6	1.836(2)	Ti2−F3×2	1.834(4)	1.833(2)	1.835(1)
Ti2−F4	1.848(2)	Ti2−F4×2	1.867(4)	1.866(1)	1.870(1)
Ti2−F7	1.872(2)	Ti2−F5	1.875(5)	1.878(2)	1.880(2)
Ti2−F3	1.875(2)				
Ti2−F5	1.893(2)				
Ti2−O4	1.910(2)	Ti2−O3	1.884(6)	1.890(2)	1.896(2)
Ti3−F8×2	1.865(2)				
Ti3−F9×2	1.874(2)				
Ti3−O3×2	1.936(2)				
P1−O1	1.491(2)	P1−O1	1.498(6)	1.492(2)	1.496(2)
P1−O2	1.553(2)	*P*1−O2×2	1.534(5)	1.531(2)	1.534(2)
P1−O3	1.551(2)				
P1−O4	1.555(2)	*P*1−O3	1.544(6)	1.537(3)	1.536(2)

Figure 1. In comparison with the characteristic absorption of the functional groups in known compounds, one may assign the main absorption bands in the spectra. The strong bands at about 1174, 998, and 954 cm^{-1} originate from tetrahedral phosphate PO_4.[31] On the other hand, the symmetric and asymmetric stretching vibration modes of the O−H band are observed around 3479 cm^{-1} in **1**, originating from trace-absorbed H_2O molecules in the compound. The bands at about 3281, 2974, 2828, and 1429 cm^{-1} in **2**, **3**, and **4** are characteristic of the symmetric, asymmetric, and bending modes for NH_4^+ ions.

Structure description. The compounds **1**, **2**, **3**, and **4** were synthesized under similar conditions; the only difference was the amines used in the systems. From the crystallographic study and IR spectra, it is clear that **1** is free of amine and the counter cations are all potassium ions. The other three compounds (from **2** to **4**) represent a gradual replacement of K^+ by NH_4^+. Therefore, the anion frameworks of the structures are identical, although they may represent different space groups ($P2_1/n$ for **1** and $P2_1/m$ for the others). The anion framework of the structures is built up with PO_4 tetrahedra and two different types of octahedra, $TiOF_5$ and TiO_2F_4. Figure 2 shows an asymmetric unit in **1**, where one could actually see that the PO_4 tetrahedron shares three oxygen atoms with the octahedral units and leaves one as a terminal. It should be noted that the fluorine atoms on $TiOF_5$ and TiO_2F_4 are, in general, terminal atoms in the fluorotitanophosphates; therefore, the fragments shown in Figure 2 may only form 1D chains through further sharing of the O2 and O3 atoms on the octahedral groups.

As shown in Table 2, the unit cell volume of **1** is twice as that of other phases. Therefore in the structure of **1**, there are 21 crystallographically distinct sites, including three titanium, one phosphorus, four oxygen, nine fluorine, and four potassium atoms. Whereas in the structures of **2**, **3**, or **4**, the crystallographically distinct sites reduce to 14, including two titaniums, one phosphorus, three oxygens, five fluorines, and three potassiums or NH_4^+. Nevertheless, the two structure types are topologically identical, and the only

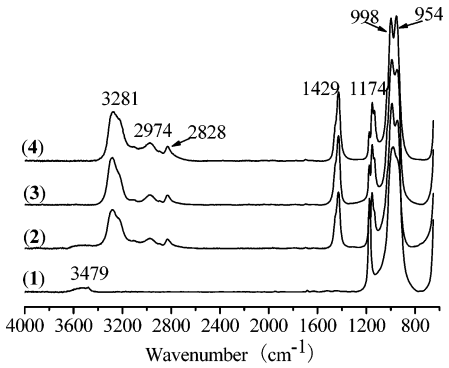

Figure 1. FTIR spectra of **1**, **2**, **3**, and **4**.

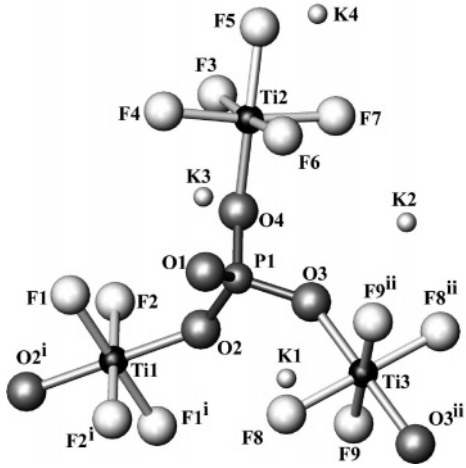

Figure 2. An asymmetric unit in the structure of **1**; symmetry codes: (i) $-1-x, -1-y, 1-z$; (ii) $-1-x, -y, 1-z$.

(31) Birsöz, B.; Baykal, A.; Toprak, M.; Köseoglu, Y. Cent. *Eur. J. Chem.* **2007**, *5*, 536−545.

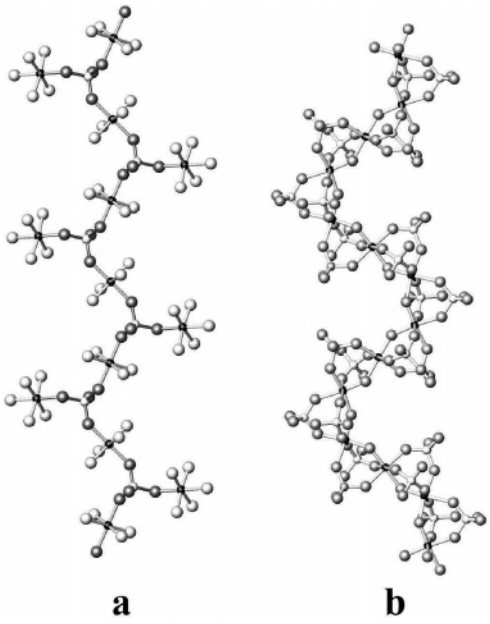

Figure 3. Structure of the titanophosphate chain in $(NH_4)_xK_{4-x}Ti_2PO_4F_9$ (a), and $[Ti_3P_6O_{27}]\cdot 5[NH_3CH_2{-}CH_2NH_3]\cdot 2H_3O$ (b).[24]

difference is that the glide plane (*n*) perpendicular to the *b* axis in **1** changes to a mirror plane in the structure of the later group. In part a of Figure 3, we show the polyhedral chain in the structure, where one can see that the PO_4 tetrahedra and TiO_2F_4 octahedra are alternatively linked, forming a $[Ti_2PO_4F_9]_n^{4n-}$ zigzag chain. Part b of Figure 3 shows another type of titanophosphate chain $[Ti_3P_6O_{27}]_n^{12n-}$ found in titanophospates,[24,25] where the TiO_6 octahedra share corners forming a $[TiO_6]_n$ octahedral chain and the PO_4 tetrahedral groups are linked to the rest of the oxygen atoms on the TiO_6 octahedra, forming three-membered [2Ti+P] rings. Comparatively, the fluorotitanophosphate chain in our compounds is unique, which is very different from the titanophosphate chain $[Ti_3P_6O_{27}]_n^{12n-}$.

Figure 4 shows the packing of the $[Ti_2PO_4F_9]_n^{4n-}$ zigzag chains in the structures. The packing fashion of the chians is exactly the same in all four compounds; however, the arrangement is more symmetric in **2**, **3**, and **4** (part b of Figure 4) than that in **1** (part a of Figure 4). In addition, the packing of the zigzag chains is rather efficient, in which the counterions, K^+ and NH_4^+, are located in the cavities among the chains. Part c of Figure 4 shows the structure projected along the *b* axis, where one can clearly see the 1D characteristic of the structure. In **2**, **3**, and **4**, when some K^+ ions were replaced by NH_4^+, a lot of hydrogen bonds formed (Supporting Information for the details), which enhance the interaction between the chains and the counterions.

Thermal Stability. Part a of Figure 5 shows TG curves of **1**, **2**, **3**, and **4** under an argon atmosphere. **1** gradually loses weight (about 1.2 wt %) up to 550 °C and, then a dramatic weight loss occurs above 700 °C. According to the mass spectra (MS) shown in part b of Figure 5, the observed species with the *m*/*z* values of 16, 17, 18 can be assigned to O, OH, H_2O, respectively, so the first weight loss is mainly due to removal of absorbed water molecules, which is consistent with the result of the IR spectrum. The large weight loss at high temperature may attribute to removal of fluorine, as indicated by MS curves $m/z = 19$. **2**, **3**, and **4** show similar thermal behavior (part a of Figure 5); the first weight loss (9.0% for **2**, 9.6% for **3**, and 10.8% for **4**) occurs between 270 °C and 600 °C. The correlation between the weight loss and the content of ammonium in the compounds implies the removal of ammonium in this temperature range. However, the observed HF and F_2 species with *m*/*z* values of 20 and 38 in the gas phase indicate that a small amount of fluorine may also be lost together with ammonium (part c of Figure 5 and also see the Supporting Information). All of these samples melt at about 610 to 630 °C, as indicated by the endothermal peak on DSC curves (Supporting Information). At the same time, the fluorine evaporates from the samples as indicated by MS curves $m/z = 19$ shown in parts b and c of Figure 5.

The X-ray diffraction patterns recorded after heating the samples at different temperatures in air are illustrated in Figure 6 for **1** and **3**. It can be seen that the framework retains up to about 500 °C for **1**, and above this temperature it collapses. The major phases in the decomposition products are $KTiOPO_4$,[32] $K_{2.67}TiO_{0.67}F_{5.33}$;[33] in addition, small quantity of $K_4Ti_{2.57}P_2O_{12}$[34] and $K_4P_2O_7$[35] are also observed. On the other hand, the framework of **3** retains up to about 420 °C, and above this temperature, it collapses and decomposes to $KTiOPO_4$, $K_{2.67}TiO_{0.67}F_{5.33}$ and anatase TiO_2.[36] In comparison with **1**, the lower thermal stability of **3** may originate from the partial substitution of ammonium, which may also be

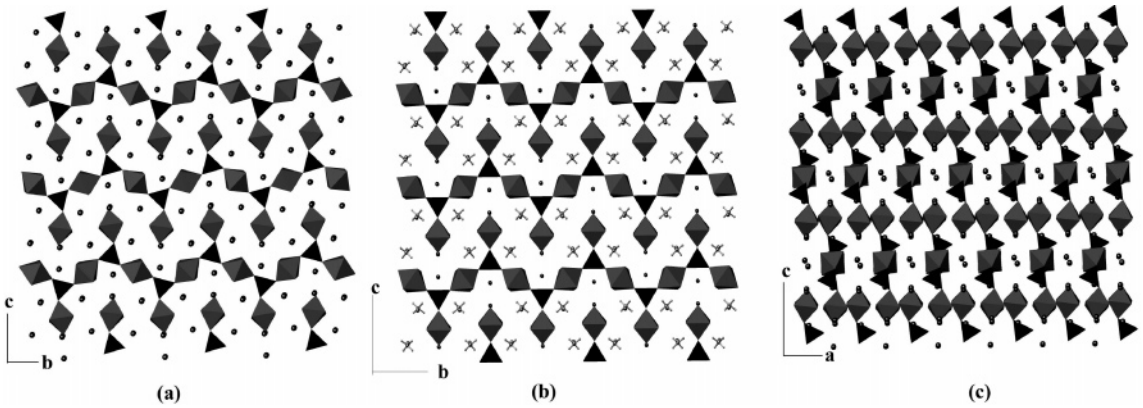

Figure 4. View of stacking of the fluorotitanophosphate chain in **1** (a) and **3** (b) along the *a* axis as well as that of **1** along the *b* axis (c).

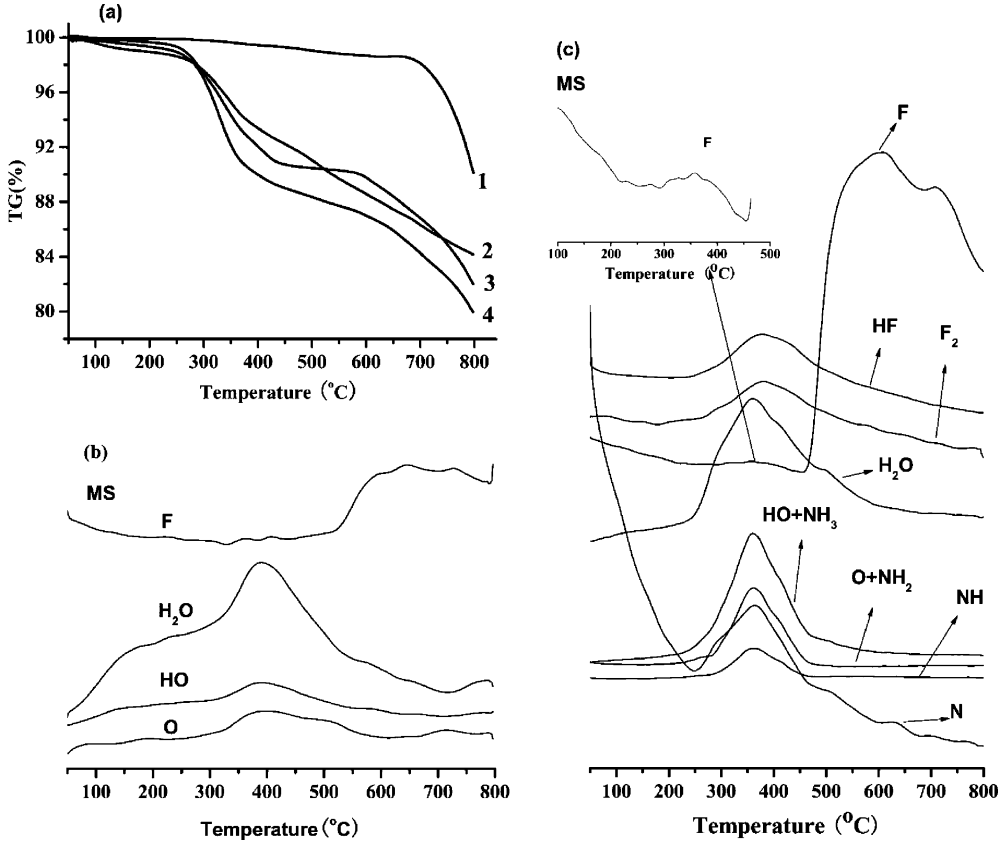

Figure 5. TG curves for **1**, **2**, **3**, and **4** (a); variation of the species (mass spectra) in the gas phase during the heating for **1** (b) and **3** (c).

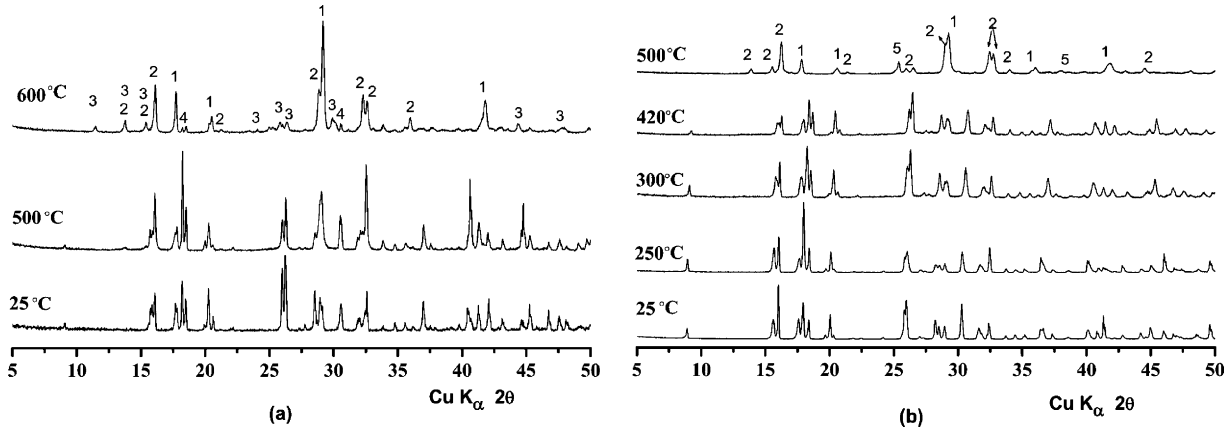

Figure 6. X-ray diffraction patterns after heating treatment at different temperature for **1** (a) and **3** (b). 1, $K_{2.67}TiO_{0.67}F_{5.33}$;[33] 2, $KTiOPO_4$;[32] 3, $K_4Ti_{2.57}P_2O_{12}$;[34] 4, $K_4P_2O_7$;[35] 5, TiO_2.[36]

responsible for the difference of minor decomposition products. Carefully examining the X-ray diffraction data in part b of Figure 6, we find that the X-ray diffraction patterns are almost unchanged below 250 °C. In fact, a small weight loss (<1%) was indeed observed for **2**, **3**, and **4**, which may be due to the loss of the surface-absorbed species. At higher temperatures, the reflections shift to higher 2θ angles, which means the unit cells shrink along with the loss of H_2O and NH_3.

Discussion and Conclusion

A series of new fluorotitanophosphate compounds have been synthesized under hydrothermal conditions. Although the reaction conditions were almost the same, the products are indeed slightly different in the content of ammonium depending on the amines in the starting materials. In addition, the structure is also slightly different, that is, the ammonium-free compound (**1**) crystallizes in a large cell (twice in volume) in the space group $P2_1/n$. Meanwhile, partial

(32) Hansen, N. K.; Protas, J.; Marnier, G. *Acta Crystallogr. B* **1991**, *47*, 660.
(33) Pausewang, G.; Schmidt, R. *Z. Anorg. Allg. Chem.* **1985**, *523*, 213.
(34) Damazyan, G. S.; Airapetyan, A. G.; Manukyan, A. L. *Arm. Khim. Zh.* **1987**, *40*,164.
(35) Brun, G. *Rev. Chim. Miner.* **1967**, *4*, 839.
(36) Horn, M.; Schwerdtfeger, C. F.; Meagher, E. P. *Z. Kristallogr.* **1972**, *136*, 273−281.

substitution of ammonium to potassium induces a structure change to a more-symmetric version. Although the structural framework remains the same, the unit cell of the structures reduces and the structures represent in the space group $P2_1/m$.

The structures of the anionic frameworks in these compounds are identical and featured in a unique 1D fluorotitanophosphate chain, consisting of alternate octahedra and tetrahedra. The formation of this unique 1D chain is obviously due to the terminal fluorine atoms on the titanium octahedra. Finally, it is noteworthy that none of the helix fluorotitanophosphate chains herein has been reported previously.

Acknowledgment. This work is supported by the National Natural Science Foundation of China (Grants 20471003 and 20531010). We gratefully acknowledge Prof. W. T. Yu and Prof. H. P. Jing for recording the X-ray powder Data.

Supporting Information Available: CIF files of the structures reported in this article; powder X-ray diffraction patterns of **1** and **3**; tables of the atomic parameters for **1**, **2**, **3** and **4**; discussions on the determination of fluorine and oxygen in the title compounds; MS curves of **2** and **4**; DSC curves of the title compounds; and the table of the hydrogen bonding for **1**, **2**, **3**, and **4**. This material is available free of charge via the Internet at http://pubs.acs.org.

IC701715K